

Collaborative Anomaly Detection

Ke Bai*
Duke University

Aonan Zhang
Bytedance Inc.

Zhizhong Li
SenseTime Research

Ricardo Henao
Duke University

Chong Wang**
Apple Inc.

Lawrence Carin
KAUST

Abstract

In recommendation systems, items are likely to be exposed to various users and we would like to learn about the familiarity of a new user with an existing item. This can be formulated as an anomaly detection (AD) problem distinguishing between “common users” (nominal) and “fresh users” (anomalous). Considering the sheer volume of items and the sparsity of user-item paired data, independently applying conventional single-task detection methods on each item quickly becomes difficult, while correlations between items are ignored. To address this multi-task anomaly detection problem, we propose collaborative anomaly detection (CAD) to jointly learn all tasks with an embedding encoding correlations among tasks. We explore CAD with conditional density estimation and conditional likelihood ratio estimation. We found that: *i*) estimating a likelihood ratio enjoys more efficient learning and yields better results than density estimation. *ii*) It is beneficial to select a small number of tasks in advance to learn a task embedding model, and then use it to warm-start all task embeddings. Consequently, these embeddings can capture correlations between tasks and generalize to new correlated tasks.

1 Introduction

User-item exposures constitute weakly labeled data when compared to strong labels such as clicks, converts (*e.g.*, user purchase items), and ratings. For in-

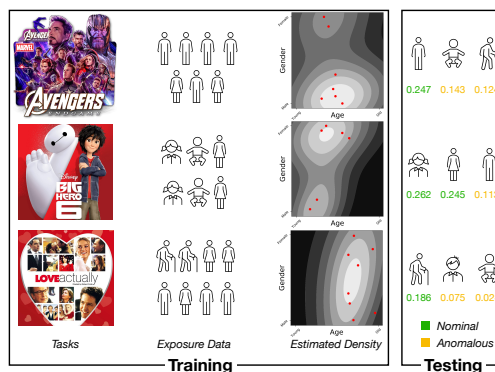


Figure 1: Each movie (task) has audiences with two real-valued features: age and gender. The goal is to learn a function for each movie to distinguish between nominal and anomalous audiences in the test set. The third column is an illustration of density estimation over the second column exposure data given the movie. The number under each cartoon portrait on the fourth column is its estimated density, describing the familiarity of this user to the movie.

stance, a user may browse an item without buying it or people may watch a video without leaving a rating. Though these situations generally do not indicate user preferences toward specific items or movies, the data generated by interactions *without action* is of interest because it is a reflection of user behavior. For example, the familiarity between the item and a user, with which the recommendation system could increase the recommendation diversity and thus improve the user experience (Kunaver and Požrl, 2017).

We formulate this familiarity estimation problem as a collection of correlated anomaly detection (AD) tasks. Figure 1 illustrates the setting using movie recommendation as an example. Assume that each movie is exposed to audiences with two features: age and gender; our goal is to determine which users in the test set are “common” (*i.e.* nominal) and which users are “fresh” (*i.e.* anomalous) for each movie. In row one of

* Work is done when the author interned at Bytedance Inc.
** Work is done when the author worked at Bytedance Inc.

Figure 1, the movie “Avengers” is mostly exposed to young adults, hence preschoolers and the elderly are anomalous to it. Alternatively, “Big Hero 6” is commonly exposed to young audiences, so preschoolers are nominal to it.

Note that the “age” and “gender” features are for illustration and evaluation only. These privacy data may not be available in reality. What’s more, the items features are usually more complex, *e.g.* image or text feature extracted from the pre-trained neural network. Simple statistics like counting over categories are not applicable.

If each movie is treated as a single AD task, then different movies (tasks) have user groups with different exposure patterns. Given that tasks share the same user pool, we will consider all tasks collectively instead of individually.

There is a plethora of research on the single-task AD problem. One can estimate the density $q(\mathbf{x})$ of nominal data or a proxy for it (Polonik et al., 1995; Tsybakov et al., 1997), and then set a threshold for the density function to discriminate nominal and anomalous data. One can also learn a mapping of nominal data from a high-dimensional space to a compact region concentrated around a pre-defined centroid, using kernel functions (Schölkopf et al., 2001; Tax and Duin, 2004) or deep neural networks (Ruff et al., 2018). Moreover, outlier exposures are informative to classify nominal *vs.* anomalous data (Hendrycks et al., 2018). There are also semi-supervised (Ruff et al., 2019), self-supervised (Hendrycks et al., 2019) and fully supervised (Ruff et al., 2020) approaches.

Yet none of the aforementioned methods are tractable to solve all tasks at once when the number of tasks is large. For example, density-based AD methods seek to estimate density functions for each movie as shown in the third column of Figure 1. However, it is inefficient to learn these conditional densities independently, due to the scarcity of exposure data for each task and the linear growth in computation costs with the number of tasks.

We propose Collaborative Anomaly Detection (CAD) to address all tasks simultaneously, where an important observation is that having a massive number of tasks facilitates the training of single tasks. In CAD, all tasks first learn their initial *task embeddings* to encode the task correlations. Then, to get the anomaly detection result, we apply the conditional likelihood ratio estimation for all tasks, where the ratio is between the distribution of exposure data from the current task and the distribution of data from all tasks. We compared our method with baselines such as conditional density estimation with Gaussian models or

normalizing flows (Rezende and Mohamed, 2015). Our study reveals: *i*) likelihood ratio estimation achieves better AD results since it benefits from the full usage of all available data, while being more efficient than density estimation when data are scarce; and *ii*) task embedding initialization is important to effectively exploit task correlations, and we utilize a warm-start strategy with the initial task embedding learned from a small subset of tasks. With these properties, CAD scales better and easily adapt to new tasks with limited exposure data. Our problem is motivated from recommendation system, the multi-task anomaly detection setting and the proposed methods can be applied to any other domains.

The remainder of the paper is organized as follows. Section 2 briefly reviews related work on AD. Section 3 introduces CAD with density estimation and likelihood ratio estimation conditioning on task embeddings. In Section 4 we discuss how to initialize task embeddings at low cost, and present the entire training procedure. Empirical results on MovieLens 1M in Section 5 show the large efficiency and accuracy gains of CAD relative to naively applying AD for each task. We also create synthesized tasks on CIFAR10, and test different CAD methods to further study their efficiency and generalization. Concluding remarks are presented in Section 6.

2 Related Work

Modern AD research has seen significant progress with the utilization of deep learning, where previously common feature mapping implementations such as kernel methods (Schölkopf et al., 2001; Tax and Duin, 2004) are replaced by deep networks (Ruff et al., 2018). Deep AD methods either aim to estimate the density of nominal data (An and Cho, 2015; Chen et al., 2017; Huang et al., 2019; Zisselman and Tamar, 2020), or to classify between nominal and anomalous data in semi-supervised, self-supervised or supervised settings (Hendrycks et al., 2018, 2019; Ruff et al., 2019, 2020).

CAD is a special case of conditional AD, where anomalous data are studied in a context such as time (Gupta et al., 2013), space (Schubert et al., 2014), or graph structures (Akoglu et al., 2015). CAD studies anomalous data in the context of each item in recommendation systems. The large number of items and complex latent structures among them make CAD considerably more challenging.

Algorithm 1 Conditional likelihood ratio estimation.

function DATASAMPLER(M, N)
 Sample N task indices $t_i \propto m^{(i)}$, where $i \in [M]$.
 Sample N instances \mathbf{x}_i given t_i as $\mathbf{x}_i \sim q^{(t_i)}(\mathbf{x})$.
 Sample N contrastive instances $\tilde{\mathbf{x}}_i \sim p(\mathbf{x})$.
return $\mathbf{t} = (t_{1:N}), \mathbf{x} = (\mathbf{x}_{1:N}), \tilde{\mathbf{x}} = (\tilde{\mathbf{x}}_{1:N})$.
end function

function ESTIMATECLR(M, e)
 Randomly initialize θ .
 Randomly initialize $e=(e^{(1)}, \dots, e^{(M)})$ if $e = \text{NONE}$.
while not converge **do**
 $\mathbf{t}, \mathbf{x}, \tilde{\mathbf{x}} = \text{DATASAMPLER}(M, N = \text{batch-size})$
 Update parameters with gradients $\nabla_{(\theta, e)} L$,
where

$$L = \frac{1}{N} \sum_{i \in [N]} \left(\log(1 + \exp(-f(\mathbf{x}_i, e^{(t_i)}, \theta))) \right. \\
 \left. + \log(1 + \exp(f(\tilde{\mathbf{x}}_i, e^{(t_i)}, \theta))) \right).$$

end while
return θ, e .
end function

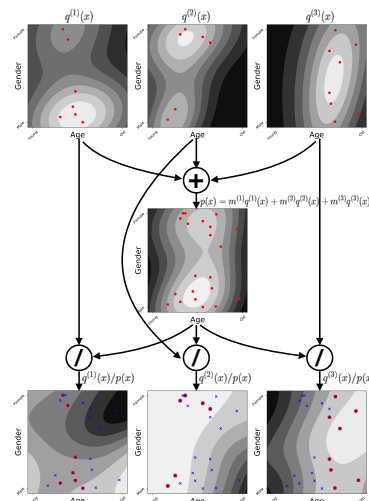


Figure 2: Colored dots are the samples. Each sample is represented by 1-d age and gender embedding. (Top) Conditional density of three tasks, (Middle) Base distribution: population density. (Bottom) Likelihood ratio. red dots illustrate the positive sample and blue dots means negative

3 Collaborative Anomaly Detection (CAD)

In CAD, each item t forms a single task, with samples \mathbf{x} from its own nominal distribution $q^{(t)}(\mathbf{x})$ representing its exposed users. Before proceeding to our main approach for CAD using conditional likelihood ratio estimation, we first present and analyze an alternative approach based on conditional density estimation, which will serve as a baseline.

3.1 CAD with conditional density estimation

In this approach, the goal is to learn a conditional density function $q(\mathbf{x}|e^{(t)})$ to approximate $q^{(t)}(\mathbf{x})$, and then identify anomalous $\mathcal{A}^{(t)}$ as data whose density is below a threshold $\mathcal{A}^{(t)} = \{\mathbf{x} \in \mathcal{X} : q(\mathbf{x}|e^{(t)}) \leq \tau\}$. Here $e^{(t)}$ is a *task embedding* vector for task t . Existing methods for conditional density estimation include Gaussian mixture models (GMM), kernel density estimators (KDE), and those based on deep neural networks such as variants of variational auto-encoders (VAE) (Pol et al., 2019), generative adversarial networks (GAN) (Mirza and Osindero, 2014), and normalizing flows (Abdelhamed et al., 2019). Section 5 will present experiment results on a variety of those methods. Below we detail the normalizing flow, as it maximizes the exact likelihood function.

Conditional normalizing flows learn task-specific invertible mappings $f_{e^{(t)}}(\mathbf{z}) : \mathcal{Z} \rightarrow \mathcal{X}$ from a simple

task-dependent Gaussian distribution $\pi_{e^{(t)}}(\mathbf{z})$ to the target distribution $q(\mathbf{x}|e^{(t)})$. The loss function is the negative log-likelihood

$$L = -\log q(\mathbf{x}|e^{(t)}) \\
 = -\log \pi_{e^{(t)}}(f_{e^{(t)}}^{-1}(\mathbf{x})) - \log \left| \det \frac{\partial f_{e^{(t)}}^{-1}(\mathbf{x})}{\partial \mathbf{z}} \right|$$

In practice, flexible normalizing flows are implemented by stacking invertible layers $f_{e^{(t)}}(\mathbf{z}) = f_{e^{(t)}}^K \circ f_{e^{(t)}}^{K-1} \circ \dots \circ f_{e^{(t)}}^1(\mathbf{z})$ (Winkler et al., 2019; Abdal et al., 2021). Our experiments suggest that conditional normalizing flows suffer from two limitations. *i*) Estimating $q^{(t)}(\mathbf{x})$ is hard since \mathbf{x} lies in a high-dimensional space and there are often only a few samples available for each task. Further, the estimated conditional density function may assign a high score for anomalous data due to the inductive bias of normalizing flows (Nalisnick et al., 2018; Kirichenko et al., 2020). *ii*) The performance of density estimation highly depends on the number of tasks.

To alleviate these issues, in Section 3.2 we consider estimating the conditional likelihood-ratio. Then in Section 4 we propose to use seed tasks to initialize the task embeddings.

3.2 CAD with conditional likelihood ratio estimation

We consider introducing a *base distribution* $p(\mathbf{x})$ from which we can sample. Then, CAD estimates the log-likelihood ratio $r^{(t)}(\mathbf{x})$ as a proxy for the density $q^{(t)}(\mathbf{x})$

$$r^{(t)}(\mathbf{x}) = \log \frac{q^{(t)}(\mathbf{x})}{p(\mathbf{x})}. \quad (1)$$

Base distribution selection As illustrated in Algorithm 1, the base distribution resembles the negative samples in the one-class classification literature (Stewart et al., 2005). A good choice for the base distribution varies with the application; however, it should be informative enough to characterize the boundary between nominal and anomalous data. In the context of recommendation systems, we choose the base distribution as the population exposure distribution $p(\mathbf{x}) = \sum_t m^{(t)} q^{(t)}(\mathbf{x})$, where $m^{(t)}$ is the proportion of users exposed to task t . Let \mathcal{P} be a feasible domain of probability measures. We can prove that

Proposition 1. $p(\mathbf{x}) = \sum_t m^{(t)} q^{(t)}(\mathbf{x})$ is optimal for minimizing the expected KL divergence

$$\min_{p(\mathbf{x}) \in \mathcal{P}} \mathbb{E}[\text{KL}(q^{(t)}|p)] = \min_{p(\mathbf{x}) \in \mathcal{P}} \sum_t \mathbb{E}_{q^{(t)}(\mathbf{x})} \left[m^{(t)} \log \frac{q^{(t)}(\mathbf{x})}{p(\mathbf{x})} \right] \quad (2)$$

Instead of using the standard density estimation defined on the Lebesgue measure \mathcal{R}^n , our likelihood ratio is a Radon–Nikodym derivative *w.r.t.* $p(\mathbf{x})$, which has two benefits. First, the likelihood ratio corrects the bias of the density by the population. For example, a moderately common sample \mathbf{x} in one task t , namely $q^{(t)}(\mathbf{x}) \approx 1$, should be marked as significant even when it is extremely rare in the population, *i.e.*, $p(\mathbf{x}) \approx 0$. Second, previous work on computational stability (Friedman et al., 2001) shows that a smaller distance between two distributions leads to more accurate likelihood-ratio estimation. Moreover, Proposition 2 shows that our choice of $p(\mathbf{x})$ is the best option under the Kullback–Leibler (KL) divergence metric. The proof can be found in the appendix.

Figure 2 demonstrates conditional density functions $q^{(t)}(\mathbf{x})$ of three tasks. To learn the density functions is arguably difficult given the scarcity of data (first row). Instead, one can estimate conditional likelihood ratios with discriminative learning, where each task has its own positive samples and some negative samples (third row) drawn from the population density function (second row). One can also observe that density functions have more modes than the likelihood ratio, thus harder to learn. This is because the population density $p(\mathbf{x})$

in this case can smooth out modes in $q^{(t)}(\mathbf{x})$ and result in simpler and smoother likelihood ratios.

Likelihood ratio estimation We learn the ratio $r^{(t)}(\mathbf{x})$ by logistic regression. Estimating the likelihood ratio for a single task t is considered first, and then we extend this to jointly learn all tasks. For each task t , we sample an observation from the nominal distribution $\mathbf{x} \sim q^{(t)}(\mathbf{x})$ as a positive example and pair it with a negative example drawn as $\tilde{\mathbf{x}} \sim p(\tilde{\mathbf{x}})$. Repeatedly doing so, we collect N contrastive pairs $(\mathbf{x}_i, y_i = 1)$ and $(\tilde{\mathbf{x}}_i, \tilde{y}_i = -1)$.

When N goes to infinity, the optimal solution θ^* for the logistic regression loss

$$L(\theta) = \frac{1}{N} \left(\sum_{i \in [N]} \log(1 + \exp(-f(\mathbf{x}_i, \theta))) + \sum_{i \in [N]} \log(1 + \exp(f(\tilde{\mathbf{x}}_i, \theta))) \right), \quad (3)$$

guarantees that $f(\mathbf{x}, \theta^*) = \log(q^{(t)}(\mathbf{x})/p(\mathbf{x}))$ for any $\mathbf{x} \in \text{supp}(q^{(t)})$ (Huang et al., 2006). The proof is in the appendix.

To learn all tasks at once, assume the number of users exposed to item t is proportional to $m^{(t)}$ and $\sum_t m^{(t)} = 1$. We sample a random user \mathbf{x} by first sampling her/his task assignment $t \propto m^{(t)}$ and then sampling $\mathbf{x} \sim q^{(t)}(\mathbf{x})$. The construction of contrastive pairs naturally extends from the single-task case. In our implementation, $f(\mathbf{x}, \mathbf{e}^{(t)}, \theta)$ is a deep neural network parameterized by θ , and each task is characterized by a vector $\mathbf{e}^{(t)}$, *i.e.* the task embedding. We demonstrate our learning framework in Algorithm 1 as ESTIMATECLR(M, \mathbf{e}), where M is the number of tasks and \mathbf{e} stands for a task embedding initialization. We use random initialization when setting $\mathbf{e} = \text{NONE}$, which is typically not the best choice in practice. We will discuss better initialization strategies in Section 4.

4 Task Embeddings Initialization

In this section, we focus on *learning* a tailored task embedding $\hat{\mathbf{e}}^{(t)}$ that can be used in initialization of Algorithm 1. We seek task embeddings with the following properties:

1. **(Correlation)** The learned initialization should capture task similarity. (Meyerson and Miikkulainen, 2020)
2. **(Generalization)** The learned task embedding models can generalize to new correlated tasks.
3. **(Efficiency)** The acquisition of learned task embeddings should be inexpensive.

Suppose there are M tasks in total. We propose to learn the task embedding $\widehat{\mathbf{e}}^{(t)}$ by first selecting $M_0 \ll M$ *seed tasks* to train a *pre-embedding model*, and then use the pre-embedding model to encode all tasks. In practice, we find that randomly selected seed tasks are representative enough to capture correlations among all tasks. This is hypothetically due to the redundancy among tasks where the inherent complexity of semantics may not be that big. We study the choice of M_0 in Section 5.2.

Train pre-embedding model with seed tasks

Without loss of generality, seed tasks are identified as task 1 to M_0 . We train a log-likelihood ratio task to get the pre-embedding model by calling $\psi, \mathbf{e} = \text{ESTIMATECLR}(M_0, \text{NONE})$ in Algorithm 1, where ψ denotes the parameters of the pre-embedding model (not related to the final conditional likelihood ratio estimation model). The returned vector \mathbf{e} is dropped, and the pre-embedding model ψ is sent to the next step.

Obtaining task embeddings initializations

Given the pre-embedding model ψ , the following basis functions are constructed,

$$\mathbf{r}(\mathbf{x}) = \left(\mathbf{r}^{(1)}(\mathbf{x}), \dots, \mathbf{r}^{(M_0)}(\mathbf{x}) \right),$$

where $\mathbf{r}^{(s)}(\mathbf{x}) = \log(q^{(s)}(\mathbf{x})/p(\mathbf{x}))$ is the log-likelihood ratio of the pre-embedding model ψ . The task embedding $\widehat{\mathbf{e}}^{(t)}$ is defined as a linear projection of $q^{(t)}(\mathbf{x})$ onto these basis functions, *i.e.*,

$$\widehat{\mathbf{e}}^{(t)} = \left(\mathbb{E}_{q^{(t)}(\mathbf{x})}[\mathbf{r}^{(1)}(\mathbf{x})], \dots, \mathbb{E}_{q^{(t)}(\mathbf{x})}[\mathbf{r}^{(M_0)}(\mathbf{x})] \right). \quad (4)$$

We independently draw $N^{(t)}$ samples $\mathbf{x}_1, \dots, \mathbf{x}_{N^{(t)}}$ from $q^{(t)}(\mathbf{x})$ to estimate $\widehat{\mathbf{e}}^{(t)}$, where each entry is estimated by $\mathbb{E}_{q^{(t)}(\mathbf{x})}[\mathbf{r}^{(s)}(\mathbf{x})] \approx \frac{1}{N^{(t)}} \sum_{n=1}^{N^{(t)}} f(\mathbf{x}_n, \mathbf{e}^{(s)}, \psi)$. This step only requires forward passing and does not involve any model updates.

After obtaining the learned task embedding initializations $\widehat{\mathbf{e}} = (\widehat{\mathbf{e}}^{(1)}, \dots, \widehat{\mathbf{e}}^{(M)})$, we can run the conditional likelihood ratio estimation as described in Section 3.2, where $\theta, \mathbf{e} = \text{ESTIMATECLR}(M, \widehat{\mathbf{e}})$. This completes the algorithm.

4.1 Interpret the learned embeddings

To informally explain why the task embedding initialization $\widehat{\mathbf{e}}^{(t)}$ in (4) captures task correlations, we treat $q^{(t)}(\mathbf{x})$ and $\mathbf{r}^{(s)}(\mathbf{x})$ as infinite-dimensional vectors by varying \mathbf{x} across its support. Random-projection theory guarantees that $\text{sim}(\widehat{\mathbf{e}}^{(t)}, \widehat{\mathbf{e}}^{(t')}) \approx \text{sim}(q^{(t)}, q^{(t')})$, when $M_0 \rightarrow \infty$ with random regular basis functions $\mathbf{r}(\mathbf{x})$ and properly chosen similarity metrics (Gottlieb

and Krauthgamer, 2015). In practice, naively generated random functions may not work well, since the random function must capture the difference of $q^{(t)}$ and $q^{(t')}$ on their support. Likelihood ratios are more reasonable to cover all supports, while still being discriminative since they are learned by contrastive pairs on the population support $\text{supp}(p(\mathbf{x}))$. In our experiments, we found the number of basis functions M_0 can be much smaller than the total number of tasks M when tasks are correlated and redundant. As we will show in experiments, the learned embedding can also generalize to previously unseen tasks.

5 Experiments

We start with experiments on the MovieLens 1M dataset to demonstrate that *i)* CAD with conditional likelihood ratio estimation achieves much better results compared to conditional density estimation; and *ii)* task embedding initialization is crucial. To further analyze these properties, we design a set of experiments on an image dataset (CIFAR10) with synthesized tasks. Unless otherwise stated, all experiments are executed on a single NVIDIA Titan Xp GPU with 12,196M Memory.

5.1 Experiments on MovieLens 1M

Problem setup The MovieLens 1M dataset contains approximately 3,900 movies and 6,040 users, together with over one million ratings (Harper and Konstan, 2015), hence 3,900 AD tasks in total, one for each movie. We ignore all rating scores and only keep the binary information of whether movies are rated (exposed) or not. We split users into training and testing sets with 8:2 ratio. The goal for each AD task is to distinguish between “common users” (nominal) and “fresh users” (anomalous) in the testing set.

Feature pre-processing In MovieLens 1M data, there are four categorical labels for users: gender (u_g), age (u_a), occupation (u_o), and zip-code (u_z); and three categorical features for items: movie id, title, and genre. We use a deep factorization-machine (Guo et al., 2017) to extract user embeddings \mathbf{x} (details in appendix) for training AD models. The detailed four categorical labels $u_{n,g}$, $u_{n,a}$, $u_{n,o}$, $u_{n,z}$ for user \mathbf{x}_n will be used for testing only.

Nominal and anomalous The definition of anomalous varies across domains (Ruff et al., 2021). We consider point anomaly in the context of recommendation systems, which aims to identify each anomalous user for an item t . An anomalous user is defined according to a specific user label. Take the label

Table 1: Anomaly detection results in terms of AUC ($\times 100$). (Left) Comparing GMM, normalizing flows, and likelihood-ratio estimation. (Right) Conditional likelihood ratio estimation with various task embedding initialization methods. * means extra knowledge is used for initialization.

METHOD	AGE	OCCUPATION	EMBEDDING INITIALIZATION	AGE	OCCUPATION
GAUSSIAN	59.5	61.5	GRAPH EMBEDDING*	80.3	68.0
NORMALIZING FLOW	60.9	58.3	HISTOGRAM EMBEDDING*	82.6	73.4
LIKELIHOOD RATIO	78.2	64.2	RANDOM INITIALIZATION	78.2	64.2
			LEARNED EMBEDDING	80.6	66.1

“age” as an example. Suppose an item t is exposed to a set of users $\mathbf{X}^{(t)} = \{\mathbf{x}_1^{(t)}, \dots, \mathbf{x}_{m^{(t)}}^{(t)}\}$, where the age of user $\mathbf{x}_n^{(t)}$ is $u_{n,a}^{(t)}$. We identify the most frequent age category $\hat{u}_a^t := \arg \max_u \sum_{n=1}^{m^{(t)}} \mathbf{1}(u_{n,a}^{(t)} = u)$ as nominal and the least frequent age category $\check{u}_a^t := \arg \min_u \sum_{n=1}^{m^{(t)}} \mathbf{1}(u_{n,a}^{(t)} = u)$ as anomalous. The AUC score is calculated on the test set by distinguishing between the nominal and anomalous users only. Since there are multiple user labels, we may report multiple AUC scores, one for each user label. In our experiments below, we test on two user labels: “Age” with 5 binned categories and “Occupation” with 21 categories.

Task filtering We remove tasks that are not eligible for AD experiments. To be precise, we first remove tasks with fewer than 100 exposures. Among the remaining tasks, we select 50% of them with the lowest user label histogram entropy, indicating nominal and anomalous are distinguishable. There are 1,629 remaining tasks after the filtering.

Methods We study CAD with the proposed conditional likelihood ratio estimation method and two conditional density estimation methods, conditional Gaussian and conditional normalizing flows. For conditional likelihood ratio estimation, we implement a 3-layer MLP, where task embeddings are concatenated to the input. For Gaussian, we use a 3-layer MLP with two output heads to map the task embedding to Gaussian mean and variance. For normalizing flows, we follow (Papamakarios et al., 2017) to stack 5 blocks, where each block is a stack of MADE (Germain et al., 2015) and BatchNorm. For all methods, we train until their losses do not decrease, and select the best checkpoints on validation and report results on testing data. Implementation details are put in appendix.

The AUC results are shown in Table 1 (left). Conditional density estimation completely fails in the CAD scenario, on both “Age” labels and on “Occupation” labels. Normalizing flows are much more flexible than Gaussian, yet still not able to discriminate the anomalous. This is because density estimation usually requires large data and model capacity for learning.

When conditioning on too many tasks, density estimation may fail to distinguish the complex correlations among tasks. This phenomenon will be further inspected in Section 5.2.

Task embedding initialization In conditional likelihood ratio estimation, task embedding $\mathbf{e}^{(t)}$ plays a critical role for data sharing across tasks, since learning one task can enhance the learning of another related task with a similar task embedding. We compare the following choices of task embedding initialization. *i) Graph Embedding*: use learned movie features through a knowledge graph base using KTUP (Cao et al., 2019) to initialize $\mathbf{e}^{(t)}$. *ii) Histogram Embedding*: when training on age labels, we calculate the histogram of users’ age labels for each task t : $\{u_{1,a}^{(t)}, \dots, u_{m^{(t)},a}^{(t)}\}$ to initialize $\mathbf{e}^{(t)}$. This is similarly done for occupations. *iii) Random Initialization*: use normal distribution to randomly initialize $\mathbf{e}^{(t)}$. *iv) Learned Embedding*: initialize $\mathbf{e}^{(t)}$ following the procedure in Section 4 with $M_0 = 100$ seed tasks. We use the same training scheme for all initialization methods. The training detail can be found in the appendix.

As shown in Table 1 (right), task embeddings with additional knowledge (marked with *) are generally superior over embeddings without such knowledge. Learned embeddings are significantly better than random embeddings, and even comparable with graph embeddings, since they attempt to uncover the connections underlying over 1,600 tasks using seed tasks.

Downstream tasks So far we have shown that our likelihood ratio can tell the anomaly data from the nominal one. It is a good measure of the familiarity between users and items. We could use this familiarity to diversify the recommendation (explore) or fit the user’s current preference (exploit). After collecting feedback like users’ reactions, satisfaction rate, or advertisements’ revenue, we can re-estimate familiarity and do the next round of recommendations. Even though this pipeline is nearly impossible to simulate given the current public dataset and evaluation metrics, we do believe that the familiarity between user and item is a necessary and meaningful signal to re-

fect the user behavior or item property. For more scenarios to use CAD, please check the Appendix.

5.2 Experimental studies on CIFAR10

The difficulty of CAD stems from the large number of correlated tasks. In this section, we synthesize AD tasks using the CIFAR10 dataset (Krizhevsky, 2009) to gain further understandings of the two phenomena: *i*) why conditional likelihood ratio estimation leads to better CAD results; and *ii*) why the learned task embeddings work better than randomly initialized embeddings. To connect with previous recommendation setting, we can treat each task as a “user”, the images in each task as “items” exposed to this user. The union of items in all tasks make up the whole dataset, which is in accordance with the recommendation that all the users share the one item set.

Problem setup Without further specification, the experiments below use the default training testing split for CIFAR10. We further split out 5,000 samples out of 60,000 training samples as a validation set. CIFAR10 has ten ground-truth categories. We will select a subset of categories, called “active categories”, to expose to a task. For evaluation, given the task index, we select all the samples from its active category as the nominal data and treat the remaining data as anomalous. We report the average AUC for all tasks on the test set.

CAD with increasing complexity We artificially create a sequence of experiments indexed by $1 \leq k \leq 4$ with an increasing number of correlated tasks. For each task in one experiment, we select k active categories out of ten. We enumerate all possible categorical combinations, resulting in C_{10}^k tasks in total. Each image is randomly exposed to only one task that is active for training. The more tasks one has, the fewer samples each task contains. We prepare four experiments with increasing complexity $k = 1, 2, 3, 4$ on two scenarios: *i*) separately learning, all tasks are learned separately; *ii*) conditional learning, all tasks are learned jointly with information sharing.

We study CAD with two (conditional) density estimation methods: Gaussian and masked autoregressive flow (MAF, (Papamakarios et al., 2017)) and compare with two modern AD methods: deep support vector data description (Deep SVDD, (Ruff et al., 2018)) and anomaly detection with contrasting shifted instances (CSI, (Tack et al., 2020)). Gaussian and MAF are implemented on 128d features extracted from an unsupervised model since they work better with high-level, dense features ((Kirichenko et al., 2020)).

Table 2 (left) shows separately learning results. There

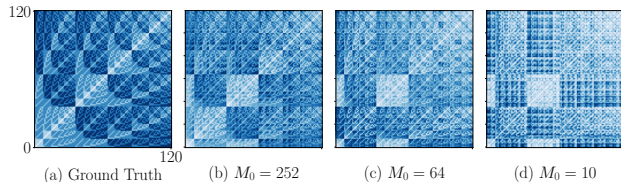


Figure 3: Pairwise similarity between 120 unseen tasks indexed by rows and columns. Lighter color represents stronger similarities. (a) Ground truth similarity measured by the number of overlapping active categories. (b-d) Cosine similarities measured by learned embeddings, by sampling (b) $M_0 = 252$, (c) $M_0 = 64$, (d) $M_0 = 10$ seed tasks.

is a sharp performance drop for Gaussian when k grows since it can only capture one mode of data distribution. MAF is more flexible than Gaussian, thus performs much better. The performance of all methods (CSI, SVDD and LRatio) trained with raw images drops quickly when the number of tasks increases since fewer samples are assigned to each task. Likelihood ratio estimation exploits samples from the base distribution, thus better discriminates nominal and anomalous both for extracted features and raw images.

Table 2 (right) lists the conditional learning results. Conditional Gaussian is generally as bad as separately trained Gaussian because of limited capacity. MAF has enough capacity to learn a single task but suffers from large k . Conditional likelihood ratio estimation performs well with the help of good task embedding and information sharing from negative samples.

Task embedding initialization We compare learned task embeddings with the following task embedding initialization approaches.

1. *Label Embedding (Label Emb.)*: a binary length L vector $\mathbf{e}^{(t)}$ where $e_\ell^{(t)} = 1$ if and only if ℓ is active for task t . Prior knowledge of active tasks is required.
2. *Pseudo Label Embedding (Pseudo Emb.)*: we cluster training data with GMM with L components. For each task t , we calculate its empirical distribution on clusters as $\mathbf{e}^{(t)}$.
3. *Random Initialization (Random Init.)*: initialize $\mathbf{e}^{(t)}$ with L -dimensional normal distributions.
4. *Learned Embedding (Learned Emb.)* ($\dim=M_0$): initialize task embeddings with M_0 pre-selected tasks following the procedure in Section 4.

We use the same architecture to integrate task embeddings, and use the training scheme for all initialization methods. Details can be found in the appendix.

As demonstrated in Table 3 (left), CAD is generally harder when handling more tasks. For two tasks t, t' ,

Table 2: Testing AUC ($\times 100$) on CIFAR10 with increasing difficulty levels $k = 1, 2, 3, 4$. The number in the brackets represents the total number of tasks. (Left) Separate learning. (Right) Conditional learning. \dagger means use pre-trained feature.

METHOD \ k	1(10)	2(45)	3(120)	4(210)	#PARAMS
GAUSSIAN \dagger	93.92 \pm 3.2	66.45 \pm 5.4	60.90 \pm 5.8	54.60 \pm 6.0	1M
MAF \dagger	91.96 \pm 1.7	90.76 \pm 2.3	83.77 \pm 2.7	79.40 \pm 1.2	0.4M
LRATIO \dagger	99.58\pm0.9	98.57\pm0.9	97.61\pm1.1	95.67\pm1.5	0.1M
DEEP SVDD	64.81 \pm 6.8	52.43 \pm 2.3	51.43 \pm 5.3	50.68 \pm 4.7	0.5M
CSI	94.28 \pm 3.8	62.53 \pm 5.3	55.78 \pm 5.6	53.78 \pm 2.3	11.5M
LRATIO	96.05\pm2.3	84.26\pm5.0	74.35\pm5.1	68.05\pm5.6	3M

METHOD \ k	1(10)	2(45)	3(120)	4(210)
GAUSSIAN \dagger	75.76	62.52	58.21	56.10
MAF \dagger	92.04	82.25	80.54	61.56
LRATIO \dagger	99.41	98.97	98.25	97.46
LRATIO	95.97	93.07	87.13	78.96

Table 3: Testing AUC ($\times 100$) on CIFAR10. (Left) Comparing various task embedding initialization methods. Label embedding uses categorical label information (marked with a *) so it has a natural advantage comparing with other methods. The best results without extra knowledge are shown in bold. (Right) To test the generalization performance of CAD, we train on a set of tasks (rows) and test on a different set of tasks (columns).

EMBEDDING INIT. \ k	2(45)	3(120)	4(210)	5(252)
LABEL EMB.* ($L=10$)	96.50	95.13	94.21	91.90
PSEUDO EMB. ($L=10$)	96.00	94.13	92.21	85.90
RANDOM INIT. ($L=10$)	95.97	93.07	87.13	78.96
LEARNED EMB. ($M_0=10$)	96.20	94.61	92.11	90.30
LEARNED EMB. ($M_0=64$)	96.43	95.06	93.45	91.40

TRAIN M \ TEST N	2(45)	3(120)	4(210)	5(252)
2 (45)	—	89.11	79.33	73.11
3 (120)	95.80	—	86.62	80.53
4 (210)	95.26	93.94	—	86.52
5 (252)	91.96	91.61	91.08	—

label distribution of samples can capture the similarities of tasks precisely, leading to good performance of *label embedding*. *Pseudo label embedding* tries to approximate label embedding, but it does not perform well when the number of tasks increases dramatically due to the limitation of GMM. *Learned embedding* with a moderate number of seed tasks can do much better than GMM, and it achieves almost the same AUC as label embeddings. *Random initialization* performs extremely poor even after fine tuning, indicating that task embedding initialization is critical in CAD.

Task generalization Surprisingly, the learned task embeddings can help identify unseen tasks fairly well without retraining or fine-tuning. To demonstrate this, we use setting $k = m$ train the pre-embedding and conditional likelihood ratio estimation models. Then we select another setting $k = n$ for testing. For each testing task t , its task embedding $e^{(t)}$ comes from the *existing* pre-embedding model. We apply $e^{(t)}$ to the *existing* conditional likelihood ratio model for testing (active categories *vs.* the rest).

Table 3 (right) shows the setup, where $m, n = 2, 3, 4, 5$ are selected as four exclusive sets of tasks (from easy to difficult) for training (indexed by each row) and testing (indexed by each column). We use $(m \rightarrow n)$ to denote training on task set m and testing on task set n . There is a generalization from training tasks to testing tasks since the testing performance is much better than random guessing (AUC = 0.5). The generalization can be attributed to two factors. First, learned embeddings capture the distribution over new task well. This will be further discussed in the next paragraph. Second, conditional likelihood ratio estimates can adapt to unseen task embeddings and make

reasonable predictions. In general, it is harder to generalize from an easy set of tasks to a difficult set of tasks (*e.g.*, $2 \rightarrow 5$) than vice versa ($5 \rightarrow 2$). This is because the easy set of tasks cannot precisely characterize the fine-grained correlations among the set of difficult tasks. However, this does not mean we can always train on hard tasks and expect to consistently achieve the best performance among all task sets since the result of $3 \rightarrow 2$ is better than $5 \rightarrow 2$, indicating the task set 3 is “closer” to task set 2 in the task semantic space, thus a better generalization performance.

Visualize generalization through task embeddings The learned task embeddings are generalizable because they can measure high-level semantics, thus express correlations among different tasks. We pre-train a task embedding model with all 252 tasks where $k = 5$ out of 10 categories are active. Then we use the task embedding model to encode another 120 unseen tasks with $k = 3$ active categories. We find that the learned task embeddings can approximate similarities between those 120 new tasks even the pre-trained network has not seen them before. Figure 3(a) shows the ground-truth similarity, measured by the number of overlapping categories between two tasks. It turns out the similarity are mainly preserved by learned embeddings in (Figure 3(b)). Learned embeddings are robust, since even a few sub-sampled indices (64 indices in Figure 3(c) and 10 indices in Figure 3(d)) can approximately preserve task similarities.

6 Conclusion and Future Work

In this paper, we studied a series of correlated anomaly detection problems with exposure data. The key to

jointly learn these AD tasks is to share information (collaborate) across them by explicitly or implicitly sharing data among tasks. Our study finds that using conditional likelihood ratio estimation with the learned task embeddings can efficiently perform CAD on MovieLens 1M with over thousands of tasks. We further studied the CIFAR10 dataset with a massive number of correlated yet different tasks, demonstrating that the proposed combination is superior to other possible choices, when data for each task is scarce, and its generalization ability.

The current work has a few limitations, which can be studied in future work. For example, the choice of seed tasks can be more selective than random picking. A full-fledged CAD may adapt to streaming data where new users and items come in real-time.

References

- Abdal, R., Zhu, P., Mitra, N. J., and Wonka, P. (2021). Styleflow: Attribute-conditioned exploration of stylegan-generated images using conditional continuous normalizing flows. *ACM Transactions on Graphics (TOG)*, 40(3):1–21.
- Abdelhamed, A., Brubaker, M. A., and Brown, M. S. (2019). Noise flow: Noise modeling with conditional normalizing flows. In *Proceedings of the IEEE/CVF International Conference on Computer Vision*, pages 3165–3173.
- Akoglu, L., Tong, H., and Koutra, D. (2015). Graph based anomaly detection and description: a survey. *Data mining and knowledge discovery*, 29(3):626–688.
- An, J. and Cho, S. (2015). Variational autoencoder based anomaly detection using reconstruction probability. *Special Lecture on IE*, 2(1):1–18.
- Cao, Y., Wang, X., He, X., Hu, Z., and Chua, T.-S. (2019). Unifying knowledge graph learning and recommendation: Towards a better understanding of user preferences. In *The world wide web conference*, pages 151–161.
- Chen, J., Sathe, S., Aggarwal, C., and Turaga, D. (2017). Outlier detection with autoencoder ensembles. In *Proceedings of the 2017 SIAM international conference on data mining*, pages 90–98. SIAM.
- Chen, T., Kornblith, S., Norouzi, M., and Hinton, G. (2020). A simple framework for contrastive learning of visual representations. In *International conference on machine learning*, pages 1597–1607. PMLR.
- Friedman, J., Hastie, T., Tibshirani, R., et al. (2001). *The elements of statistical learning*, volume 1. Springer series in statistics New York.
- Germain, M., Gregor, K., Murray, I., and Larochelle, H. (2015). Made: Masked autoencoder for distribution estimation. In *International Conference on Machine Learning*, pages 881–889. PMLR.
- Gottlieb, L.-A. and Krauthgamer, R. (2015). A non-linear approach to dimension reduction. *Discrete & Computational Geometry*, 54(2):291–315.
- Guo, H., Tang, R., Ye, Y., Li, Z., and He, X. (2017). Deepfm: a factorization-machine based neural network for ctr prediction. *arXiv preprint arXiv:1703.04247*.
- Gupta, M., Gao, J., Aggarwal, C. C., and Han, J. (2013). Outlier detection for temporal data: A survey. *IEEE Transactions on Knowledge and data Engineering*, 26(9):2250–2267.
- Harper, F. M. and Konstan, J. A. (2015). The movie-lens datasets: History and context. *Acm transactions on interactive intelligent systems (tiis)*, 5(4):1–19.
- Hendrycks, D., Mazeika, M., and Dietterich, T. (2018). Deep anomaly detection with outlier exposure. *arXiv preprint arXiv:1812.04606*.
- Hendrycks, D., Mazeika, M., Kadavath, S., and Song, D. (2019). Using self-supervised learning can improve model robustness and uncertainty. In *Advances in Neural Information Processing Systems*, pages 15663–15674.
- Huang, C., Cao, J., Ye, F., Li, M., Zhang, Y., and Lu, C. (2019). Inverse-transform autoencoder for anomaly detection. *arXiv preprint arXiv:1911.10676*.
- Huang, J., Gretton, A., Borgwardt, K., Schölkopf, B., and Smola, A. (2006). Correcting sample selection bias by unlabeled data. *Advances in neural information processing systems*, 19:601–608.
- Kirichenko, P., Izmailov, P., and Wilson, A. G. (2020). Why normalizing flows fail to detect out-of-distribution data. *arXiv preprint arXiv:2006.08545*.
- Krizhevsky, A. (2009). Learning multiple layers of features from tiny images. Technical report.
- Kunaver, M. and Požrl, T. (2017). Diversity in recommender systems—a survey. *Knowledge-based systems*, 123:154–162.
- Meyerson, E. and Miikkulainen, R. (2020). The traveling observer model: Multi-task learning through spatial variable embeddings. *arXiv preprint arXiv:2010.02354*.
- Mirza, M. and Osindero, S. (2014). Conditional generative adversarial nets. *arXiv preprint arXiv:1411.1784*.

- Nalisnick, E., Matsukawa, A., Teh, Y. W., Gorur, D., and Lakshminarayanan, B. (2018). Do deep generative models know what they don't know? *arXiv preprint arXiv:1810.09136*.
- Papamakarios, G., Pavlakou, T., and Murray, I. (2017). Masked autoregressive flow for density estimation. *arXiv preprint arXiv:1705.07057*.
- Pol, A. A., Berger, V., Germain, C., Cerminara, G., and Pierini, M. (2019). Anomaly detection with conditional variational autoencoders. In *2019 18th IEEE International Conference On Machine Learning And Applications (ICMLA)*, pages 1651–1657. IEEE.
- Polonik, W. et al. (1995). Measuring mass concentrations and estimating density contour clusters—an excess mass approach. *The Annals of Statistics*, 23(3):855–881.
- Rezende, D. and Mohamed, S. (2015). Variational inference with normalizing flows. In *International Conference on Machine Learning*, pages 1530–1538. PMLR.
- Ruff, L., Kauffmann, J. R., Vandermeulen, R. A., Montavon, G., Samek, W., Kloft, M., Dietterich, T. G., and Müller, K.-R. (2021). A unifying review of deep and shallow anomaly detection. *Proceedings of the IEEE*.
- Ruff, L., Vandermeulen, R., Goernitz, N., Deecke, L., Siddiqui, S. A., Binder, A., Müller, E., and Kloft, M. (2018). Deep one-class classification. In *International conference on machine learning*, pages 4393–4402.
- Ruff, L., Vandermeulen, R. A., Franks, B. J., Müller, K.-R., and Kloft, M. (2020). Rethinking assumptions in deep anomaly detection. *arXiv preprint arXiv:2006.00339*.
- Ruff, L., Vandermeulen, R. A., Görnitz, N., Binder, A., Müller, E., Müller, K.-R., and Kloft, M. (2019). Deep semi-supervised anomaly detection. *arXiv preprint arXiv:1906.02694*.
- Schölkopf, B., Platt, J. C., Shawe-Taylor, J., Smola, A. J., and Williamson, R. C. (2001). Estimating the support of a high-dimensional distribution. *Neural computation*, 13(7):1443–1471.
- Schubert, E., Zimek, A., and Kriegel, H.-P. (2014). Local outlier detection reconsidered: a generalized view on locality with applications to spatial, video, and network outlier detection. *Data mining and knowledge discovery*, 28(1):190–237.
- Steinwart, I., Hush, D., and Scovel, C. (2005). A classification framework for anomaly detection. *Journal of Machine Learning Research*, 6(2).
- Tack, J., Mo, S., Jeong, J., and Shin, J. (2020). Csi: Novelty detection via contrastive learning on distributionally shifted instances. *arXiv preprint arXiv:2007.08176*.
- Tax, D. M. and Duin, R. P. (2004). Support vector data description. *Machine learning*, 54(1):45–66.
- Tsybakov, A. B. et al. (1997). On nonparametric estimation of density level sets. *The Annals of Statistics*, 25(3):948–969.
- Winkler, C., Worrall, D., Hoogeboom, E., and Welling, M. (2019). Learning likelihoods with conditional normalizing flows. *arXiv preprint arXiv:1912.00042*.
- Zisselman, E. and Tamar, A. (2020). Deep residual flow for out of distribution detection. In *Proceedings of the IEEE/CVF Conference on Computer Vision and Pattern Recognition*, pages 13994–14003.

A Log-likelihood Ratio Estimation

A.1 Proof of Proposition 1 in Section 3.2.

Proposition 2. $p(\mathbf{x}) = \sum_t m^{(t)} q^{(t)}(\mathbf{x})$ is optimal for minimizing the expected KL divergence

$$\min_{p(\mathbf{x}) \in \mathcal{P}} \mathbb{E}[\text{KL}(q^{(t)}|p)] = \min_{p(\mathbf{x}) \in \mathcal{P}} \sum_t \mathbb{E}_{q^{(t)}(\mathbf{x})} \left[m^{(t)} \log \frac{q^{(t)}(\mathbf{x})}{p(\mathbf{x})} \right] \quad (5)$$

Proof. Expanding the expectation over tasks. We get

$$\mathbb{E}[\text{KL}(q^{(t)}|p)] = \sum_t m^{(t)} [\text{KL}(q^{(t)}|p)]. \quad (6)$$

We need to solve a minimization problem with constraints:

$$\begin{aligned} \min_{p(\mathbf{x}) \in \mathcal{P}} \quad & \sum_t \mathbb{E}_{q^{(t)}(\mathbf{x})} \left[m^{(t)} \log \frac{q^{(t)}(\mathbf{x})}{p(\mathbf{x})} \right] \\ \text{s.t.} \quad & \int p(\mathbf{x}) d\mathbf{x} = 1. \end{aligned} \quad (7)$$

With the Lagrange multiplier λ , we need to find function $p(\mathbf{x})$ to minimize the Lagrangian

$$\sum_t \mathbb{E}_{q^{(t)}(\mathbf{x})} \left[m^{(t)} \log \frac{q^{(t)}(\mathbf{x})}{p(\mathbf{x})} \right] + \lambda \left(\int p(\mathbf{x}) d\mathbf{x} - 1 \right). \quad (8)$$

After removing additive terms unrelated to $p(\mathbf{x})$, we get

$$\int \left(\sum_t -m^{(t)} q^{(t)}(\mathbf{x}) \log p(\mathbf{x}) + \lambda p(\mathbf{x}) \right) d\mathbf{x}. \quad (9)$$

In the calculus of variations, $p(\mathbf{x})$ is varied by adding a function $\delta p(\mathbf{x})$ to it with ϵ multiplier, where $\epsilon \rightarrow 0$:

$$\int \left(\sum_t -m^{(t)} q^{(t)}(\mathbf{x}) \log (p(\mathbf{x}) + \epsilon \delta p(\mathbf{x})) + \lambda (p(\mathbf{x}) + \epsilon \delta p(\mathbf{x})) \right) d\mathbf{x}. \quad (10)$$

The change in the value to first order in ϵ should be zero. By taking derivative w.r.t. ϵ and let $\epsilon = 0$, we get

$$\int \left(\sum_t -m^{(t)} q^{(t)}(\mathbf{x}) \frac{\delta p(\mathbf{x})}{p(\mathbf{x})} + \lambda (\delta p(\mathbf{x})) \right) d\mathbf{x} = 0. \quad (11)$$

The above equation is valid for any function $\delta p(\mathbf{x})$

$$\lambda - \frac{1}{p(\mathbf{x})} \sum_t m^{(t)} q^{(t)}(\mathbf{x}) = 0. \quad (12)$$

After reordering terms, we get

$$p(\mathbf{x}) = \frac{1}{\lambda} \sum_t m^{(t)} q^{(t)}(\mathbf{x}). \quad (13)$$

Since $\int p(\mathbf{x}) = 1$ and $\sum_t m^{(t)} = 1$, taking the integral over \mathbf{x} on both sides of Equation 13 permits $\lambda = 1$. Finally, we get

$$p(\mathbf{x}) = \sum_t m^{(t)} q^{(t)}(\mathbf{x}). \quad (14)$$

This concludes our proof. \square

A.2 Proof of the optimal solution to Equation 3

Suppose we have two distributions $q(\mathbf{x})$ and $p(\mathbf{x})$, their log-likelihood ratio $r(\mathbf{x}) = \log(q(\mathbf{x})/p(\mathbf{x}))$ can be estimated as follows.

First, we independently draw N samples from $q(\mathbf{x})$ and label those data as positive: $\{\mathbf{x}_i, y_i = 1\}_{i=1}^N$. Similarly we draw N samples from $p(\mathbf{x})$ as label those as negative: $\{\mathbf{x}_i, y_i = -1\}_{i=N+1}^{2N}$. We combine all positive samples and negative samples into one dataset $D = \{\mathbf{x}_i, y_i\}_{i=1}^{2N}$. In the limit of $N \rightarrow \infty$, the mixed distribution satisfies:

$$p(y = 1|\mathbf{x}) = \frac{q(\mathbf{x})}{p(\mathbf{x}) + q(\mathbf{x})}. \quad (15)$$

Then we train a binary classifier on the mixed dataset D . Suppose we are using a linear logistic regression model:

$$\hat{p}(y|\mathbf{x}; \boldsymbol{\theta}) = \sigma(y \cdot \boldsymbol{\theta}^\top \mathbf{x}), \quad (16)$$

where σ is the sigmoid function:

$$\sigma(z) = \frac{1}{1 + e^{-z}}. \quad (17)$$

Then

$$\begin{aligned} \log \frac{q(\mathbf{x})}{p(\mathbf{x})} &= \log \frac{p(y = 1|\mathbf{x})}{1 - p(y = 1|\mathbf{x})} \\ &\approx \log \frac{\hat{p}(y = 1|\mathbf{x}; \boldsymbol{\theta})}{1 - \hat{p}(y = 1|\mathbf{x}; \boldsymbol{\theta})} \\ &= \log \frac{\sigma(\boldsymbol{\theta}^\top \mathbf{x})}{\sigma(-\boldsymbol{\theta}^\top \mathbf{x})} \\ &= \boldsymbol{\theta}^\top \mathbf{x}. \end{aligned} \quad (18)$$

One can use a non-linear model implemented with a neural network $f(\mathbf{x}, \boldsymbol{\theta})$ to get a better estimation of the log-likelihood ratio.

B Conditional Normalizing Flow

B.1 Feature extractors.

A good image generator implemented with normalizing flows is not necessary a good out-of-distribution detector, since normalizing flows tend to capture pixel correlations rather than semantics during training (Kirichenko et al., 2020). Moreover, normalizing flow models for image generation often requires a large number of parameters and long training time, which is not-applicable when the number of tasks is large.

To resolve above issues, we use pre-trained low-dimensional features instead of raw images to train normalizing flows. The features are extracted using unsupervised contrastive learning (Chen et al., 2020) with a ResNet-18 as the backbone model. The training accuracy on the extracted features is 90.2% with a linear classifier, demonstrating high feature quality. The unsupervised learning procedure guarantees that the extracted feature does not leak its label information while preserving image semantics.

B.2 Two ways to implement conditional normalizing flows.

In the following, we use $\mathbf{e}^{(t)}$ to represent task-specific information, which can involve in the prior π and the invertible mapping f as follows:

$$L = -\log q(\mathbf{x}|\mathbf{e}^{(t)}) = -\log \pi_{\mathbf{e}^{(t)}}(f_{\mathbf{e}^{(t)}}^{-1}(\mathbf{x})) - \log \left| \det \frac{\partial f_{\mathbf{e}^{(t)}}^{-1}(\mathbf{x})}{\partial \mathbf{x}} \right|$$

Task-specific priors For un-conditional normalizing flows, the prior π is usually set as a centered isotropic Gaussian. In our conditional case, each task t has its task-specific Gaussian prior $\pi_{\mathbf{e}^{(t)}}$ with a uniformly sampled mean vector and an identity covariance matrix.

Task-specific mappings MAF uses Masked Autoencoder for Distribution Estimation (MADE) as its building blocks. The core idea behind MADE is autoregressive flow, which generates data recursively by

$$x_i = u_i \exp \alpha_i + \mu_i$$

Where $\mu_i = f(\mathbf{x}_{1:i-1})$, $\alpha_i = g(\mathbf{x}_{1:i-1})$. \mathbf{u} is randomly generated from the previous layer or the prior distribution. In our MADE implementation, function f and g are both 4-layer autoregressive fully connected layer with masking. The task specific features are combined with the output of each MADE layer by scaling and biasing, i.e. $f_{\mathbf{e}^{(t)}} = f \odot \tanh(e_{scale}^{(t)}) + \tanh(e_{bias}^{(t)})$. The hyperbolic tangent function is used to stabilize

the training, and it can be replaced with deep neural networks. $e_{scale}^{(t)}$ and $e_{bias}^{(t)}$ are trainable task embeddings. These parameters are shared among different i in one layer. The same technique also applies to function g . For more details on MAF, please refer to the origin paper Germain et al. (2015); Papamakarios et al. (2017).

Our implementation refers to two Github codebases ^{1,2}.

C Real scenarios for CAD

D Training Details

In this section, we give full descriptions of models in our experiments.

D.1 MNIST and CIFAR10

Figure 4 demonstrates the network structure of the likelihood ratio estimation model ($f(\mathbf{x}, \mathbf{e}, \theta)$ in Algorithm 1) for MNIST and CIFAR10. We resize all MNIST figures from their original size 28×28 to 32×32 to align with CIFAR10 figure sizes. The data augmentations include random crop with padding (Pad the image to 40×40 with zeros, then randomly choice a 32×32 area) and random horizontal flip. We normalize pixels for each channel such that their mean equals zero and variance equals to one.

The pre-embedding model uses a similar feature extractor, followed by a fully connected layer mapping from feature dimension $c_dim * 8$ to 256. Then M_0 fully connected output heads are used to predict the likelihood ratio for M_0 seed tasks.

D.2 MovieLens 1M

D.2.1 Feature Extractor

Unlike CIFAR10 and MNIST where each image has its raw pixel representation, the user feature is implicitly represented by the interaction between movies and users. We treat MovieLens as a click-through rating prediction dataset and use a deep factorization-machine (Guo et al., 2017) to extract user embeddings \mathbf{x} . After training the factorization model, we use the trained embedding layer to extract features of each user. During the training process, all users are visible to the model, so we can get the feature of each user.

¹pytorch-normalizing-flows: <https://github.com/karpathy/pytorch-normalizing-flows>.

²pytorch-flows: <https://github.com/ikostrikov/pytorch-flows>

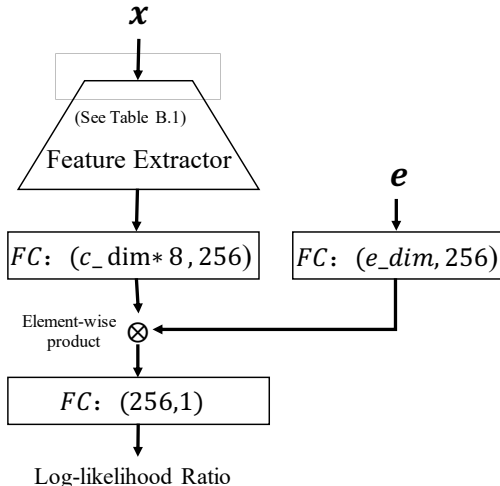


Figure 4: The framework we use to train MNIST and CIFAR10. \mathbf{x} denotes the input matrix. \mathbf{e} is the task embedding. FC represents the fully connected layer. The brackets followed by contains the dimension of its input and output. e_{dim} is the dimension of the task embedding. The definition of c_{dim} and the detail of feature extractor can be found in Table 4.

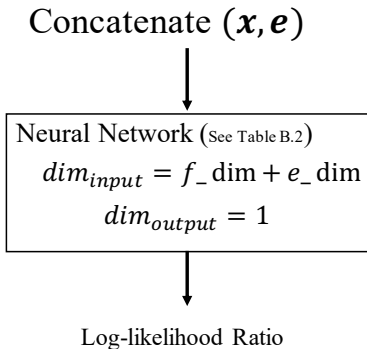


Figure 5: The framework we use to train MovieLens 1M. The definition of f_{dim} , e_{dim} and the detail of neural network can be found in Table 5.

We implement this method using code from Cao et al. (2019).

D.2.2 Hyper-parameters

Figure 5 demonstrates the network structure of the likelihood ratio estimation model ($f(\mathbf{x}, \mathbf{e}, \theta)$ in Algorithm 1) for MovieLens 1M dataset. The pre-embedding model uses the same network structure. The only difference is that we change the way to integrate task embeddings from adding them to the input to adding M_0 output heads in the pre-embedding model.

Table 4: The network structure of feature extractor for CIFAR10 and MNIST. Each operation contains four parts: (kernel size, stride, padding size), number of output channel, batch normalization (BN) and activation function. In our setting, we use $c_{dim} = 64$. The output size is a three-dimensional vector: (width, height, channel). The input channel is 3 for CIFAR10 and 1 for MNIST.

Stage	Operation	Output Size
Input	Data Augmentation	(32,32,3 or 1)
1	(4, 2, 1), c_{dim} , BN, ReLU	(16, 16, c_{dim})
2	(4, 2, 1), $c_{dim} * 2$, BN, ReLU	(8, 8, $c_{dim} * 2$)
3	(5, 1, 0), $c_{dim} * 4$, BN, ReLU	(4, 4, $c_{dim} * 4$)
4	(4, 1, 0), $c_{dim} * 8$, BN,	(1,1, $c_{dim} * 8$)

Table 5: The network structure of logistic regression for MovieLens 1M. Each operation contains three parts: (input size, output size) of fully connected layer, activation function and dropout rate. f_{dim} represents the dimension of input data. e_{dim} is the dimension of the task embedding. We use $f_{dim}=100$, $e_{dim} = 16$.

Stage	Operation
1	($f_{dim} + e_{dim}$, 32), ReLU, Dropout (0.5)
2	(32, 32), ReLU, Dropout (0.5)
3	(32, 16), ReLU, Dropout (0.3)
4	(16, 1), Linear, No Dropout

E More results on MNIST

Similar as Table 3 (left) in the main text for the CIFAR10 dataset, we study different task embedding initialization methods (see Section 5.2 in the main text for definitions of those task embeddings) on the MNIST dataset with two CAD settings where $k = 4$ with $C_{10}^4 = 210$ tasks, and $k = 5$ with $C_{10}^5 = 252$ tasks. We skip the setting with $k = 2$ and $k = 3$ since those settings are too simple such that every method we tried can get almost 100% AUC. The results is shown in Table 6.

Table 6: Testing AUC ($\times 100$) on MNIST. Label embedding uses prior knowledge (ground truth label) so it has a natural advantage comparing with other methods (Note that the first method “label embedding” uses extra knowledge and is marked with *. The best results without extra knowledge are shown in bold.).

EMBEDDING INIT. \ K (#TASKS)	4 (210)	5 (252)
LABEL EMBEDDING*	99.88	99.67
PSEUDO LABEL EMBEDDING	97.88	98.67
RANDOM INITIALIZATION	97.02	86.80
LEARNED EMBEDDING ($M_0 = 10$)	98.88	99.67
LEARNED EMBEDDING ($M_0 = 64$)	99.93	99.90